Aalborg Universitet

AALBORG UNIVERSITY
DENMARK

Enhanced Reliability of 1500-V Photovoltaic Inverters with Junction Temperature Limit Control

He, Jinkui; Sangwongwanich, Ariya; Yang, Yongheng; Iannuzzo, Francesco

Enhanced Reliability of 1500-V Photovoltaic Inverters with Junction Temperature Limit Control

Jinkui He*, Ariya Sangwongwanich*, Yongheng Yang**, and Francesco Iannuzzo*

*Department of Energy Technology, Aalborg University, Pontoppidanstraede 111, Aalborg East 9220, Denmark
**College of Electrical Engineering, Zhejiang University, Zheda Rd. 38, Hangzhou 310027, China
Email: jhe@et.aau.dk, ars@et.aau.dk, yang_yh@zju.edu.cn, fia@et.aau.dk

Abstract—This paper investigates the potential to enhance the reliability of 1500-V single-stage photovoltaic (PV) inverters with a junction temperature control strategy, where PV inverters can operate either in the maximum power point tracking mode or a junction temperature limit control mode depending on the thermal stress on the inverter power devices. With this, the junction temperature of the power devices in the PV inverter can be kept below a certain limit during operation. The effectiveness (i.e., reliability enhancement) of the proposed junction temperature control on the PV inverter reliability is demonstrated on a 60-kW three-level 1500-V PV inverter installed in Denmark. Case study results indicate that the proposed control has a high ability to enhance the inverter reliability, where the lifetime of the highest stressed power device can be extended to a large extent, while incurring a negligible reduction in energy yield.

Index Terms—Photovoltaic (PV) inverters, maximum power point tracking (MPPT), lifetime, reliability.

I. INTRODUCTION

For large-scale photovoltaic (PV) power plants, 1500-V PV systems are increasingly employed compared to the traditional 1000-V ones with the objective of achieving lower installation costs [1]–[4]. In general, these PV power plants need to be designed to last longer than 20 years. In this context, apart from the PV panels with the 1500-V technology, the PV inverters will play a crucial role in the efficient and reliable energy conversion in PV systems [5]. With the objective of reducing the cost of solar energy, the two targets of the PV inverters, i.e., maximum energy yield and long lifetime, in fact, may counteract one another [6], [7]. In such a case, special considerations (in terms of PV inverter design and control) are required to effectively reduce the levelized cost of energy (LCOE) in PV systems [8], [9].

The reliability of 1500-V PV inverters can be enhanced with an integration of DC-coupled battery energy storage system (BESS) [10], [11]. However, in addition to the considerable investments, the design of a reliable DC-DC converter for the BESS is challenging due to the increased voltage stress for 1500-V applications. Alternatively, possibilities seen from the control perspective have been discussed in prior-art research. For example, for the grid-connected PV inverters with two-stage conversion, a DC-link voltage control method for efficiency and reliability improvement was proposed in [12], where the minimum DC-link voltage ensuring proper power transfer is calculated in real-time to reduce the stresses on the power devices. In [6], a hybrid maximum power point tracking

(MPPT) method was proposed for the DC/DC converter of PV systems, which can limit the positive junction temperature gradient in the presence of fast irradiance variations. Furthermore, the constant power generation (CPG) control can effectively avoid overloading of PV inverters during peak solar irradiance periods. At the same time, the CPG control can reduce the thermal loading of PV inverters, as presented in [7], [13]. Nevertheless, the CPG control may not fully utilize the inverter capacity for a given power limit level (e.g., in the case of a high PV power input at low ambient temperatures). Besides, the aforementioned control concepts are mainly for two-stage PV converters, and provide reliability evaluation for PV inverters. However, the issues on the single-stage PV inverters have not been fully studied yet, especially for 1500-V applications, where multi-level inverters are normally employed. On the contrary, most of the previous discussions are focused on two-level inverters, where the uneven distribution of loading among the power devices is not involved.

The junction temperature is a key index for the reliability of power devices, which is determined by the variations of ambient temperature and the heating-cooling processes during power variations (reflecting mission profile characteristics) [14]. A reduction of junction temperature (mean value and/or cycle amplitude), by means of power control/regulation, can increase the reliability of the system without additional costs for enhancing the components or the converter design [9], [15].

Considering the above, this paper proposes a junction temperature control concept to improve the reliability of 1500-V PV inverters. The proposed control strategy is a combination of an MPPT control strategy and a junction temperature limit control scheme, which are alternated in operation based on the mission profile conditions (i.e., solar irradiance and ambient temperature) of the PV systems. Fig. 1 illustrates the benefit of the proposed control, where the maximum mean junction temperature is limited to 90 °C during operation. In contrast, the mean junction temperature will be close to 100 °C when operating in the conventional MPPT mode. It should be mentioned that the selection of the temperature limit reference should consider the tradeoff between the reliability performance and the system energy yield, which is different from the overloading protection which operates to avoid overheating the power device.

The rest of this paper is structured as follows. Section II describes the proposed junction temperature control strategy,
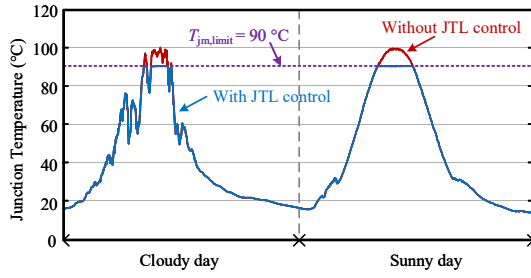
Fig. 1. Mean junction temperature of the inverter power device with/without junction temperature limit (JTL) control.
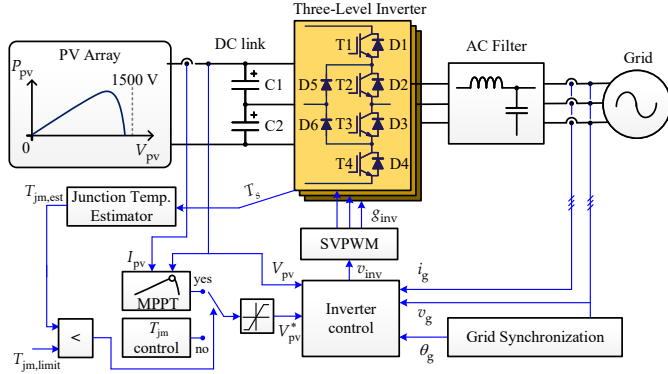

Fig. 2. Schematic and control diagram of a single-stage 1500-V PV inverter with the proposed junction temperature control strategy: T_s – heatsink temperature, $T_{jm,est}$ – estimated mean junction temperature, $T_{jm,limit}$ – mean junction temperature limit.

TABLE I
PV SYSTEM PARAMETERS.

| PV inverter specifications	
Nominal power P_{nom}	60 kW
Overload factor	1.1
Power factor $\cos(\varphi)$	1.0
Grid line-to-line RMS voltage V_{LL}	400 V
Grid frequency f_g	50 Hz
Switching frequency f_{sw}	10 kHz
Power device type	39MLI12T4V1 [16]
Voltage rating / Current rating	1200 V / 150 A
Heatsink thermal impedance $R_{th(s-a)}$	0.04 K/W
Modulation method	Space vector pulse width modulation (SVPWM)
PV panel configuration	
PV panel part number	JKM380M-72-V [17]
PV panel quantity (in series / in parallel)	27 / 6
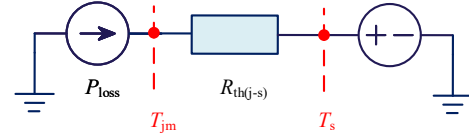
Fig. 3. Thermal model for the mean junction temperature estimator, which is referenced to the heatsink temperature T_s.

as well as the dynamical behavior of the system in the case of irradiance changing. After that, the procedures for analyzing the inverter reliability are provided in Section III, along with a case study considering a real mission profile recorded in Denmark. Finally, Section IV gives the concluding remarks.

II. JUNCTION TEMPERATURE LIMIT CONTROL

Fig. 2 depicts the considered 1500-V PV system, as well as the overall control structure. Here, a 60-kW single-stage three-level inverter is employed as the interfacing unit between the PV array and the power grid. The system parameters are given in Table I.

As shown in Fig. 2, the first step of the control algorithm is to obtain the junction temperature with a junction temperature estimator. Here, as shown in Fig. 3, only the junction-to-heatsink thermal resistance is considered since the target output of the estimator is the mean junction temperature of a certain power device (i.e., IGBT or diode). Accordingly, the mean junction temperature can be estimated as

$$T_{jm,est} = R_{th(j-s)} \cdot P_{loss} + T_s \tag{1}$$

where $R_{th(j-s)}$ is the junction-to-heatsink thermal resistance, P_{loss} is the total power losses (i.e., conduction and switching losses) of the power device, and T_s is the heatsink temperature of the power module.

It should be mentioned that the power devices employed in the three-level I-type inverter have unequal power losses and

thus thermal stresses. Normally, under inverter operation and with unity power factor, the outer IGBTs (e.g., T1 and T4 in Fig. 2) will be the most stressed devices [18]. However, for the considered system, the thermal stress of the clamping diodes is slightly higher than that of the outer IGBTs due to the relatively lower modulation indexes [19]. As the reliability performance of the PV inverter is limited by the most stressed devices, in this paper, the target of the proposed control is to limit the thermal loading of the clamping diodes. The conduction and switching loss of the clamping diode can be modeled as [20]

$$P_{cond} = \frac{\hat{I}}{12\pi} \cdot [V_{f0} \cdot [12 + 3M[(2\varphi - \pi)\cos(\varphi) - 2\sin(\varphi)]] + r_f \hat{I} \cdot [3\pi - 4M(1 + \cos^2(\varphi))]] \tag{2}$$

$$P_{sw} = f_{sw} \cdot E_{sw(ref)} \cdot \left(\frac{\hat{I}}{I_{ref}}\right)^{k_i} \cdot \left(\frac{v_{CC}}{V_{ref}}\right)^{k_v} \cdot \left[\frac{1}{2\pi}(1 + \cos(\varphi))\right] \cdot G_i \tag{3}$$

in which $\hat{I}$ represents the peak value of device current, V_{f0} is the forward threshold voltage, M is the modulation index, φ is the conduction angle, r_f is the on-state slope resistance,
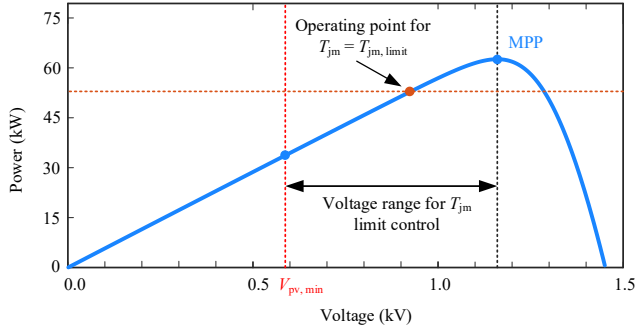
Fig. 4. Operational principle of the PV system with the junction temperature limit control, where the operating point of the PV array is regulated to the left side of the maximum power point (MPP) to ensure $T_{jm} \leq T_{jm,limit}$.

$E_{sw(ref)}$ is the switching energy reference value, V_{ref} and I_{ref} are the blocking voltage and current of diode, respectively, which represent the test conditions for the switching loss measurement, v_{CC} represents the actual blocking voltage that is being applied, $k_v = 0.6$ and $k_i = 0.6$ are the voltage and current exponents for estimating the switching losses, and $G_i = 1.15$ is the adaptation factor for the non-linear semiconductor characteristics. More details regarding the power loss calculation for the power devices within the three-level I-type inverter are provided in [20].

Generally, modern power modules incorporate a thermistor for heatsink temperature monitoring. Along with a proper measurement of thermal resistance/impedance from junction to thermistor sensor, it is possible to estimate the junction temperature with the module-integrated low-bandwidth temperature sensor [21], [22].

In order to realize the junction temperature limit control, the PV output power should be reduced (i.e., below the available PV power) to bring the mean junction temperature down. This is implemented by regulating of the PV voltage, which can be expressed as (4), as it is also demonstrated in Fig. 4

$$V_{pv}^* = \begin{cases} V_{MPPT}, & \text{when } T_{jm} \leq T_{jm,limit} \\ V_{pv} - V_{step}, & \text{when } T_{jm} > T_{jm,limit} \end{cases} \quad (4)$$

where V_{MPPT} represents the reference voltage for MPPT operation, V_{step} is the perturbation step voltage, T_{jm} is the mean junction temperature of the most stressed device, and $T_{jm,limit}$ is the reference value for junction temperature limit control. Here, only the left-side of the MPP is considered for simplicity, thus, the voltage range for the junction limit control is from MPP to the lower PV voltage limit for inverter operation (determined by the grid voltage).

According to Fig. 2 and (4), in case of a breach of the temperature limit, the PV voltage reference will be decreased to reduce the output power, and relieve the thermal loading of PV inverter eventually. The temperature limit can be selected by considering the tradeoff between the thermal performance and the annual energy yield, which will be discussed in Section III. When the mean junction temperature is lower than the limit reference, the system enters into MPPT control mode and the temperature limit control is disabled. A flowchart
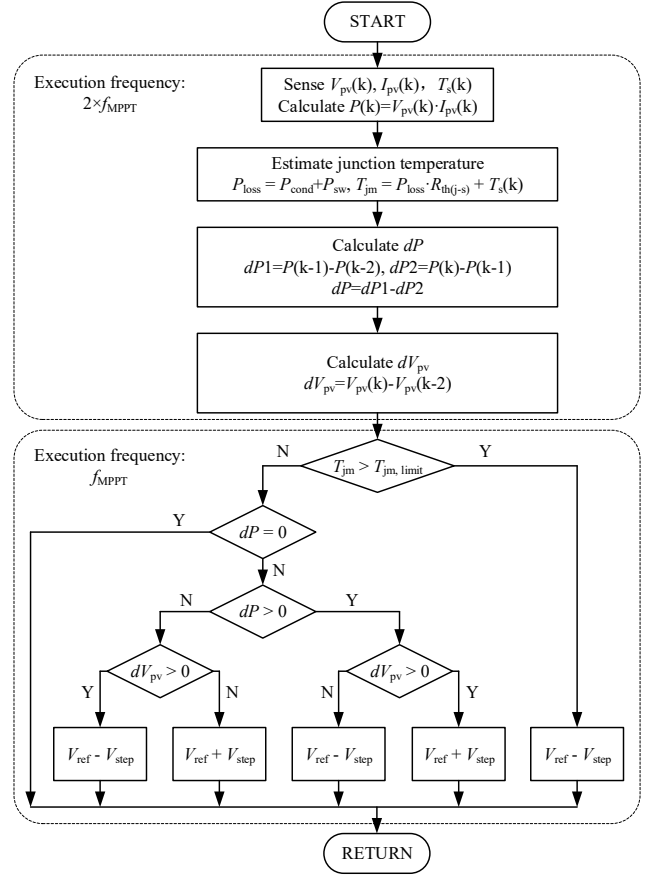

Fig. 5. Flowchart of the proposed mean junction temperature limit control, where f_{MPPT} is the execution frequency of the perturbation.

shows the realization of the junction temperature limit control in Fig. 5, which is based on an improved Perturb and Observe (P&O) method presented in [23], referred to as dP-P&O. Compared with the standard P&O method [24], the dP-P&O method performs an extra measurement of PV output power in the middle of the perturbation period to obtain the power variation only caused by the perturbation and avoid the influence of the fast irradiance change. The optimal choice of the perturbation period and size for the standard P&O method is also valid for the proposed power control, which can be found in [25]. Notably, the junction-to-case thermal impedance of the considered IGBT module has a relatively small time constant, which means that, after each duty-cycle perturbation, the mean junction temperature can reach the steady-state before the next temperature estimation. Consequently, as shown in Fig. 5, the same perturbation size is applied when a violation of the temperature limit occurs.

In order to verify the effectiveness of the proposed junction temperature control strategy, an irradiance ramp change is used. As shown in Fig. 6, the irradiance increases linearly from 0.7 kW/m^2 to 0.9 kW/m^2, remains this level for 5 s, and then back to 0.7 kW/m^2. The period for increasing and decreasing the irradiance is 5 s. The considered ambient temperature is 25 °C, which will determine the DC-link voltage of MPP.
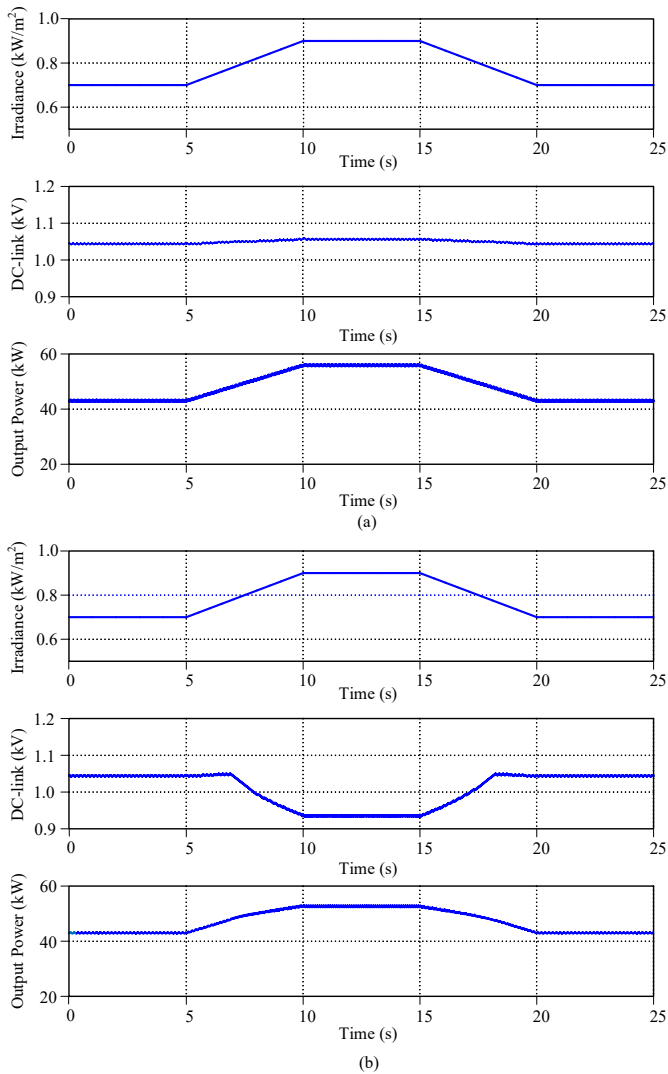
Fig. 6. DC-link voltage and output power variations of the PV inverter under a trapezoidal irradiance profile: (a) without the junction temperature limit control and (b) with the junction temperature limit control.
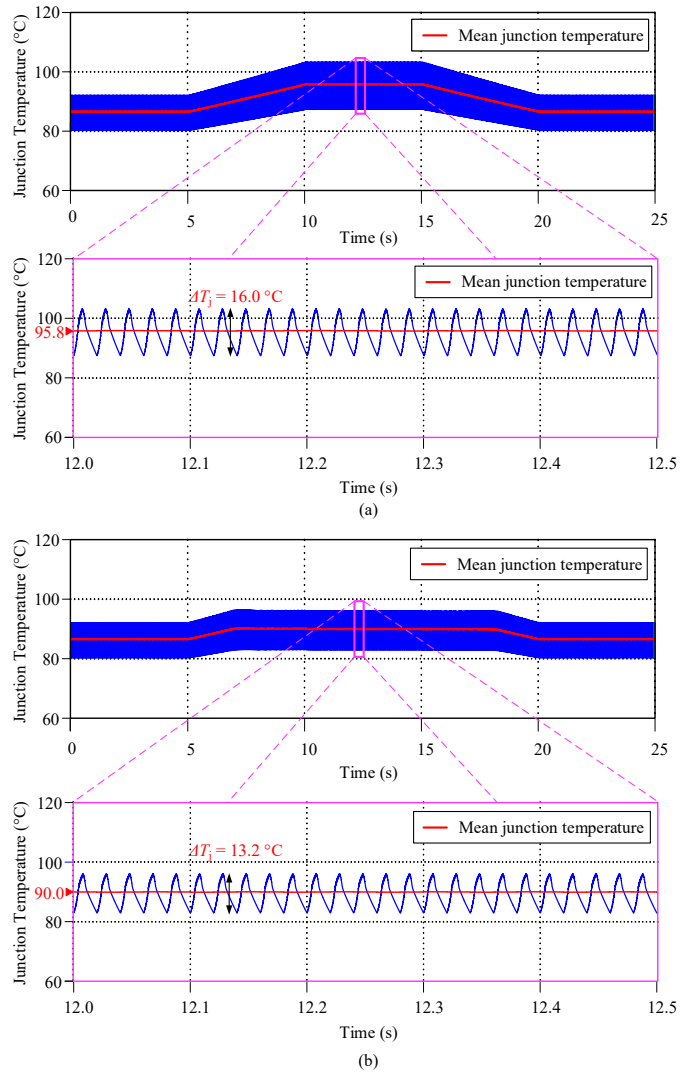

Fig. 7. Thermal stress of the power device (i.e., clamping diode) within the PV inverter under a trapezoidal irradiance profile: (a) without the junction temperature limit control and (b) with the junction temperature limit control.

The heatsink temperature is set to be at a fixed temperature of 60 °C, having considered its large thermal capacitance and the short duration of the irradiance variation. The MPPT execution frequency and voltage perturbation size, in both cases, are 25 Hz and 2 V, respectively.

As it can be seen in Fig. 6(a), without the junction temperature limit control, the DC-link voltage is slightly increased/decreased with the irradiance increase/decrease, and the output power is proportional to the irradiance changes. Consequently, as shown in Fig. 7(a), the mean junction temperature of the highest stressed power device, i.e., the clamping diode (e.g., D5/D6 in Fig. 2) is increased from 85.7 °C to 95.8 °C along with the irradiance increase. In contrast, as shown in Fig. 7(b), when applying the proposed temperature control, the DC-link voltage has come down to reduce the output power, and the maximum mean junction temperature is holding at the temperature limit reference, i.e., 90 °C. It

should be noted that the temperature cycle amplitude is also down to 13.2 °C, while it is 16 °C in the case of MPPT control. The impact of the temperature limit control on the reliability performance of the PV inverter as well as the energy yield will be discussed in the next section.

III. RELIABILITY ASSESSMENT

Real operating conditions are considered in this paper to evaluate the inverter reliability. A one-year variations of ambient temperature and solar irradiance recorded in Denmark with a sampling rate of 1 minute per sample is applied as the mission profiles of the considered PV system, which are shown in Fig. 8 [26]. Correspondingly, the reliability assessment of power devices requires the thermal loading results obtained from a long-term simulation. In this case study, based on the mission profile-based reliability assessment method in [3], a modified method is developed for translating mission profile to device thermal loading, as shown in Fig. 9. The idea
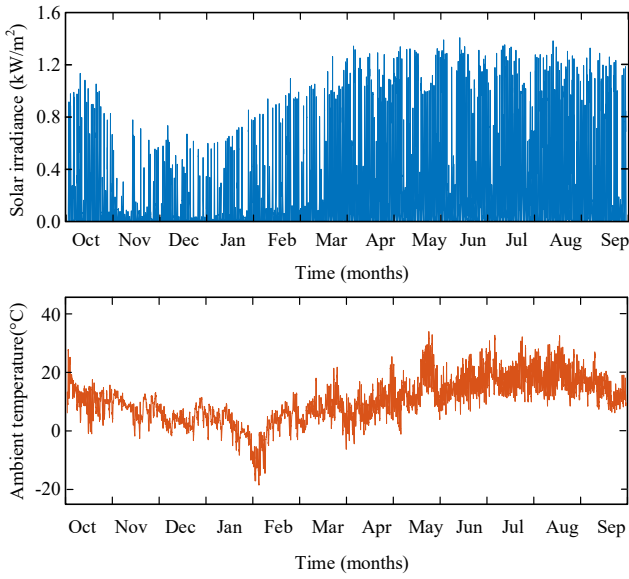
Fig. 8. One-year variations of solar irradiance and ambient temperature recorded in Denmark with a sampling rate of 1 minute per sample.

behind this method is to include maximum mean junction temperature limitation and DC-link voltage variation in the translation procedure instead of a single MPPT operation mode and constant DC-link voltage. First, based on the PV curves under different ambient temperatures, the possible operating range of the inverter (e.g., PV power levels, from 50% to 100% maximum power, and the corresponding PV voltages) is obtained. Then, considering the maximum allowable inverter input power for a certain limit of maximum mean junction temperature under different dc-link voltages, the operating point for the proposed control can be obtained. Afterward, the thermal loading of the power devices can be estimated based on the thermal loading look-up tables, which are obtained from electro-thermal simulations of the inverter model under different dc-link voltages.

Fig. 10 shows the one-year thermal loadings of the clamping diode (e.g., D5/D6 in Fig. 2). It can be observed in Fig. 10 that, when a 90 °C maximum junction temperature limit is applied, the clamping diodes experience much lower thermal stresses compared to the MPPT control, indicating a considerable potential for lifetime extension. This is achieved at the cost of a reduction of the inverter output power, as shown in Fig. 11, where the output power with the proposed control is less than that with the MPPT control during the summer days (e.g., May to Sep.). Consequently, a tradeoff should be considered between the lifetime extension and the reduction in energy yield, which will be analyzed in the following.

With the obtained long-term thermal loadings, the inverter lifetime can be estimated based on the lifetime model of the power devices. In this case study, the empirical lifetime model proposed in [27] is adopted. It provides the relationship between the number of cycles to failure N_f and certain thermal stress conditions considering the power device specifications, which is expressed as [27]
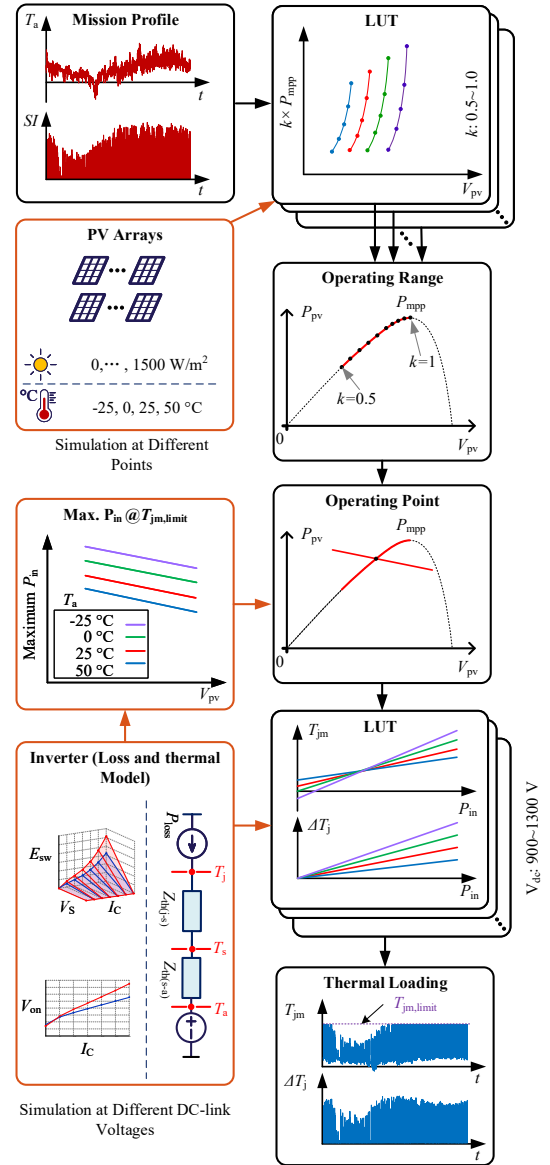

Fig. 9. Mission profile translation procedure: SI – solar irradiance, T_a – ambient temperature, P_{pv} – PV output power, LUT – lookup table, T_{jm} – mean junction temperature, and ΔT_j – cycle amplitude of the junction temperature, T_j, T_s – junction and heatsink temperature, E_{sw} – switching loss, V_{on} – voltage drop, V_s – DC-link voltage, I_c – collect current.

$$N_f = A \cdot (\Delta T_j)^{-\beta_1} \cdot \exp\left(\frac{\beta_2}{T_{j(min)} + 273}\right) \cdot t_{on}^{\beta_3} \cdot I^{\beta_4} \cdot V^{\beta_5} \cdot D^{\beta_6}$$

(5)

in which the technology fact A, cycle amplitude of junction temperature ΔT_j, minimum junction temperature $T_{j(min)}$, heating time t_{on}, current per bond wire I, voltage class V, and bond wire diameter D have been considered. These parameters are listed in Table II. More details for the lifetime model have been discussed in [27]. Besides, considering the irregular variation of thermal loading profiles, a rainflow counting method is applied to categorize the actual thermal cycles into several
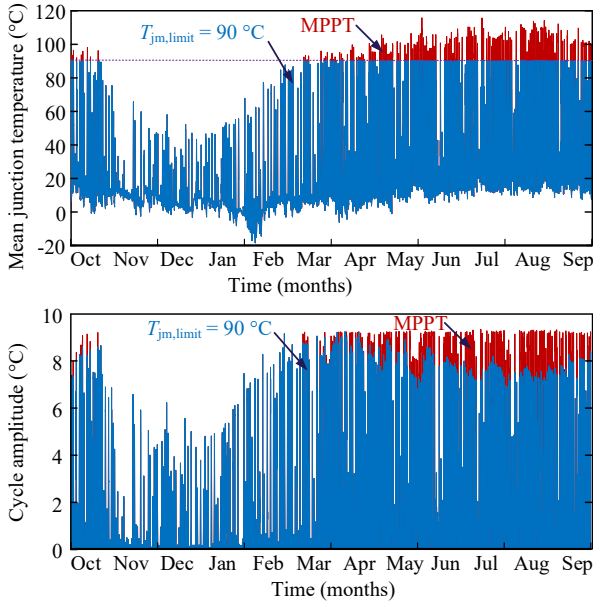
Fig. 10. Mean junction temperature T_{jm} and cycle amplitude ΔT_j of the clamping diode D5 (referring to Fig. 2) with and without junction temperature limit control under the Denmark mission profile.
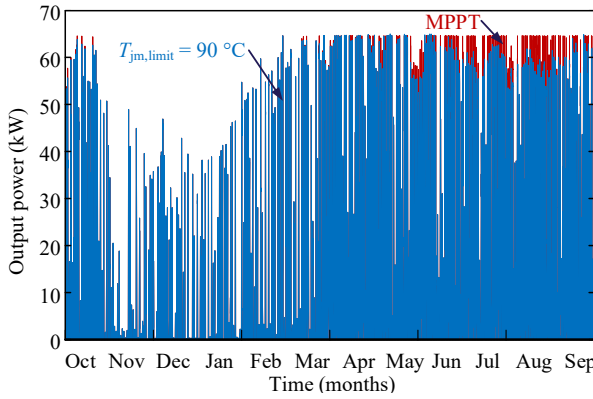

Fig. 11. Comparison of the inverter output power with and without junction temperature limit control.

group of regular cycles [28]. After this, the power device lifetime consumption (LC) is accumulated linearly according to the Miner's rule [29].and the one-year LC is calculated according to

$$LC = \sum_i \frac{n_i}{(N_f)_i} \quad (6)$$

in which n_i represents the number of temperature cycles with a certain thermal stress, and $(N_f)_i$ represents the number of cycles to failure under the same thermal stress as for n_i, which is calculated by (5).

For comparing the lifetime performance, a normalized lifetime (LF) is defined as

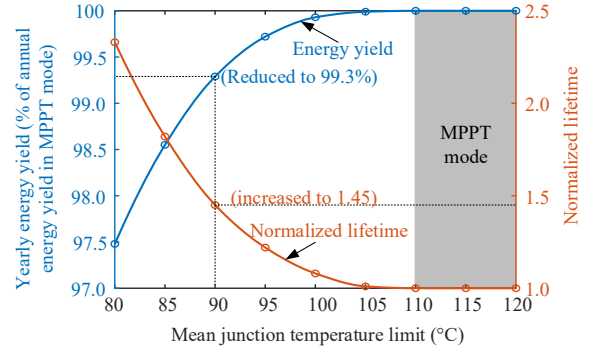$$LF = \frac{1}{\overline{LC}} \quad (7)$$

Fig. 12. Yearly PV system energy yield and normalized lifetime of the inverter clamping diode with the proposed control concept.

where $\overline{LC}$ represents the LC of the power devices with the proposed control strategy normalized to that with conventional MPPT scheme.

The value of LF has been computed for various mean junction temperature limits, as well as the corresponding energy yield, as shown in Fig. 12. For the considered case study, it can be observed in Fig. 12 that, a considerable lifetime extension of the power device can be achieved when the maximum junction temperature is limited below 100 °C. Moreover, according to Fig. 12, the energy loss is increased with the decreasing of the mean junction temperature limit, which should be considered when selecting the limit reference. It is true that Fig. 12 can be extended to lower limit reference (e.g., < 80 °C) and find the maximum value of the product of energy yield and lifetime. However, the component-level analysis is not enough to determine the tradeoff between the reliability and energy yield, which should be measured with the consideration of the system-level reliability and will be the future work. The above results suggest that the junction temperature limit control can extend the lifetime of the most stressed device to a large extent at the cost of a slight reduction in energy yield.

TABLE II
PARAMETERS OF THE EMPIRICAL LIFETIME MODEL IN [27].

Parameter	Value / Test condition
Technology factor A	9.34×10^{14}
Cycle amplitude ΔT_j	$45\,K \leq \Delta T_j \leq 150\,K$
Minimum junction temperature $T_{j(min)}$	$20\,°C \leq T_{j(min)} \leq 120\,°C$
Heating time t_{on}	$1\,s \leq t_{on} \leq 15\,s$
Current per bond wire I	3 A to 23 A
Voltage class/100 V	6 V to 33 V
Bond wire diameter D	75 μm to 500 μm
Coefficient β_1-β_3	{-4.416, 1285, -0.463}
Coefficient β_4-β_6	{-0.716, -0.761, -0.5}

IV. CONCLUSION

In this paper, a reliability enhancement strategy for 1500-V PV inverters through junction temperature limit control was

proposed considering mission profiles. The proposed junction temperature control strategy is able to limit the maximum junction temperature, and thus reduce the temperature variations. With this, the PV inverter lifetime can be extended due to the reduced thermal stresses. The thermal stress reduction is compromised with a certain energy loss. The impact of the proposed junction temperature limit control on the reliability and energy yield of the PV system is analyzed with the mission profiles of a 60-kW three-level 1500-V inverter installed in Denmark. The corresponding case study results indicate that, by restricting the maximum mean junction temperature to 90 °C, the lifetime of the highest stressed power device is extended to 1.45 times of that in the MPPT operation mode at the price of 0.7% energy yield reduction.

REFERENCES

[1] R. Inzunza, R. Okuyama, T. Tanaka, and M. Kinoshita, "Development of a 1500Vdc photovoltaic inverter for utility-scale PV power plants," in *Proc. IFEEC*, pp. 1–4, Nov 2015.

[2] E. Serban, M. Ordonez, and C. Pondiche, "DC-bus voltage range extension in 1500 V photovoltaic inverters," *IEEE J. Emerg. Sel. Top. Power Electron.*, vol. 3, no. 4, pp. 901–917, Dec. 2015.

[3] B. Stevanović, D. Serrano, M. Vasić, P. Alou, J. A. Oliver, and J. A. Cobos, "Highly efficient, full ZVS, hybrid, multilevel DC/DC topology for two-stage grid-connected 1500-V PV system with employed 900-V SiC devices," *IEEE J. Emerg. Sel. Top. Power Electron.*, vol. 7, no. 2, pp. 811–832, Jun. 2019.

[4] E. Gkoutioudi, P. Bakas, and A. Marinopoulos, "Comparison of PV systems with maximum DC voltage 1000V and 1500V," in *Proc. IEEE PVSC*, pp. 2873–2878, 2013.

[5] J. He, A. Sangwongwanich, Y. Yang, and F. Iannuzzo, "Lifetime evaluation of three-level inverters for 1500-V photovoltaic systems," *IEEE J. Emerg. Sel. Top. Power Electron.*, 2020, Early Access.

[6] M. Andresen, G. Buticchi, and M. Liserre, "Thermal stress analysis and MPPT optimization of photovoltaic systems," *IEEE Trans. Ind. Electron.*, vol. 63, no. 8, pp. 4889–4898, 2016.

[7] Y. Yang, H. Wang, F. Blaabjerg, and T. Kerekes, "A hybrid power control concept for PV inverters with reduced thermal loading," *IEEE Trans. Power Electron.*, vol. 29, no. 12, pp. 6271–6275, 2014.

[8] Y. Yang, A. Sangwongwanich, and F. Blaabjerg, "Design for reliability of power electronics for grid-connected photovoltaic systems," *CPSS Trans. Power Electron. Applicat.*, vol. 1, no. 1, pp. 92–103, Dec. 2016.

[9] M. Andresen, K. Ma, G. Buticchi, J. Falck, F. Blaabjerg, and M. Liserre, "Junction temperature control for more reliable power electronics," *IEEE Trans. Power Electron.*, vol. 33, no. 1, pp. 765–776, 2018.

[10] A. Sangwongwanich, G. Angenendt, S. Zurmühlen, Y. Yang, D. Sera, D. U. Sauer, and F. Blaabjerg, "Enhancing PV inverter reliability with battery system control strategy," *CPSS Trans. Power Electron. Appl.*, vol. 3, no. 2, pp. 93–101, 2018.

[11] J. He, Y. Yang, and D. Vinnikov, "Energy storage for 1500 V photovoltaic systems: A comparative reliability analysis of DC- and AC-coupling," *Energies*, vol. 13, no. 13, 2020. [Online]. Available: https://www.mdpi.com/1996-1073/13/13/3355

[12] J. M. S. Callegari, A. F. Cupertino, V. d. N. Ferreira, and H. A. Pereira, "Minimum DC-link voltage control for efficiency and reliability improvement in PV inverters," *IEEE Trans. Power Electron.*, vol. 36, no. 5, pp. 5512–5520, 2021.

[13] J. He, A. Sangwongwanich, Y. Yang, and F. Iannuzzo, "Thermal performance evaluation of 1500-VDC photovoltaic inverters under constant power generation operation," in *Proc. IEEE CPERE*, pp. 579–583, 2019.

[14] J. Kuprat, C. H. Van der Broeck, M. Andresen, S. Kalker, R. W. De Doncker, and M. Liserre, "Research on active thermal control: Actual status and future trends special issue commemorating 40 years of WEMPEC, 2021," *IEEE J. Emerg. Sel. Top. Power Electron.*, 2021, Early Access.

[15] D. A. Murdock, J. E. R. Torres, J. J. Connors, and R. D. Lorenz, "Active thermal control of power electronic modules," *IEEE Trans. Ind. Appl.*, vol. 42, no. 2, pp. 552–558, 2006.

[16] Semikron. IGBT Module MiniSKiiP II 3: SKiiP 39MLI12T4V1. (2021). [Online]. Available: https://www.semikron.com/products/product-classes/igbt-modules/detail/skiip-39mli12t4v1-25230510.html

[17] Jinko. JKM380M-72-V Solar Panel. (2019). [Online]. Available: http://jinkosolar.com.au/wp-content/uploads/2019/03/EaglePerc-JKM360-380M-72-V-A1-EN.pdf

[18] M. Schweizer, T. Friedli, and J. W. Kolar, "Comparative evaluation of advanced three-phase three-level inverter/converter topologies against two-level systems," *IEEE Trans. Ind. Electron.*, vol. 60, no. 12, pp. 5515–5527, Dec. 2013.

[19] K. Ma and F. Blaabjerg, "Modulation methods for three-level neutral-point-clamped inverter achieving stress redistribution under moderate modulation index," *IEEE Trans. Power Electron.*, vol. 31, no. 1, pp. 5–10, 2016.

[20] Semikron. 3L NPC & TNPC Topology. (2015). [Online]. Available: https://www.semikron.com/service-support/downloads/detail/semikron-application-note-3l-npc-tnpc-topology-en-2015-10-12-rev-05.html

[21] Semikron. Calculating Junction Temperature using a Module Temperature Sensor. (2020). [Online]. Available: https://www.semikron.com

[22] M. Andresen, M. Schloh, G. Buticchi, and M. Liserre, "Computational light junction temperature estimator for active thermal control," in *Proc. ECCE*, pp. 1–7, 2016.

[23] D. Sera, R. Teodorescu, J. Hantschel, and M. Knoll, "Optimized maximum power point tracker for fast-changing environmental conditions," *IEEE Trans. Ind. Electron.*, vol. 55, no. 7, pp. 2629–2637, 2008.

[24] T. Esram and P. L. Chapman, "Comparison of photovoltaic array maximum power point tracking techniques," *IEEE Trans. Energy Convers.*, vol. 22, no. 2, pp. 439–449, 2007.

[25] N. Femia, G. Petrone, G. Spagnuolo, and M. Vitelli, "Optimization of perturb and observe maximum power point tracking method," *IEEE Trans. Power Electron.*, vol. 20, no. 4, pp. 963–973, 2005.

[26] Y. Yang, H. Wang, F. Blaabjerg, and K. Ma, "Mission profile based multi-disciplinary analysis of power modules in single-phase transformerless photovoltaic inverters," in *Proc. EPE*, pp. 1–10, Sep. 2013.

[27] R. Bayerer, T. Herrmann, T. Licht, J. Lutz, and M. Feller, "Model for power cycling lifetime of IGBT modules - various factors influencing lifetime," in *Proc. Int. Conf. Integr. Power Syst.*, pp. 1–6, Mar. 2008.

[28] H. Huang and P. A. Mawby, "A lifetime estimation technique for voltage source inverters," *IEEE Trans. Power Electron.*, vol. 28, no. 8, pp. 4113–4119, Aug. 2013.

[29] M. Miner, "Cumulative damage in fatigue," *J. Appl. Mech.*, vol. 12, pp. 159–164, 1945.